# Investigation of Lithium Precipitates in Germanium Crystals by Anomalous X-Ray Transmission

HELMUT F. WENZL **

Solid State Division, Oak Ridge National Laboratory Oak Ridge, Tennessee 37830

(Z. Naturforsch. **26 a**, 495—501 [1971]; eingegangen am 21. November 1970)

*Herrn Prof. H. Maier-Leibnitz zum 60. Geburtstag gewidmet*

The precipitation of lithium dissolved in germanium crystals and the re-solution of the precipitates during heating has been studied by means of anomalous transmission of x-rays. The effective absorption coefficient depends sensitively on the spacial distribution of lithium interstitials, and is enhanced enormously if pair correlations increase, as is the case during clustering. On the basis of Dederichs' theory and knowledge about the Geli phase diagram, the experiments provide relations between concentration and radius of the precipitates, distortion parameters, and average and local concentration of lithium interstitials.

## 1. Introduction

X-rays can penetrate perfect crystals with an effective absorption coefficient $\mu_{\text{eff}}$ which is much smaller than the normal one, $\mu_0$, by exciting dynamical wave fields (anomalous x-ray transmission, Borrmann effect)[1]. In a nearly perfect crystal in which the lattice is distorted by thermal vibrations or lattice defects, $\mu_{\text{eff}}$ is enhanced by an additional term $\mu^*$. $\mu^*$ depends sensitively on the spacial distribution of foreign atoms or self defects and the strength of their distortion fields and is enhanced enormously if pair correlations between the defects increase[2], as is the case during clustering or precipitation or near critical points. We have utilized this fact in an investigation of the precipitation of lithium interstitials in germanium crystals. The properties of the GeLi system are important especially for the production and performance of germanium particle detectors[3]. Besides this more practical aspect, the GeLi system provides a convenient exampte of a two component system in which large changes in the pair correlation between the atoms of one of the components are possible.

Precipitation has been studied in homogeneously doped samples with lithium as the principal impurity (unlike the compensated detector systems). As methods we used anomalous x-ray diffraction in Laue geometry[4], diffraction in Bragg geometry[4], electron microscopy, and electrical conductivity. Usually, the electrical conductivity at the surface of the sample has been used as a measure of the concentration of single lithium interstitials[5]. The anomalous x-ray transmission on the other hand is most sensitive to lithium clusters. In this sense the two methods are complementary. The x-ray method, though, has the advantage of allowing measurements of bulk properties of the crystals at any temperature.

## 2. Samples

Most of the crystals were obtained from FOX[5], who had doped them at 425 °C with lithium and studied the precipitation as a function of time, after quenching them to room temperature, by measuring the electrical conductivity. Figure 1 shows an example of the results.

For the x-ray measurements, discs 1 cm diameter and thickness $t_0$ (see Table 2) with {111}-faces were cut with a diamond saw, lapped, etched [5 minutes in (1 HF + 3 $HNO_3$)-solution] and rinsed in distilled water.

For the electron microscopy blocks of $3 \times 3 \times 0.2$ mm³ size were cut with a diamond saw, the edges were masked with teflon tape, then etched in (1 HF +

* Research sponsored by the U.S. Atomic Energy Commission under contract with Union Carbide Corporation.

** On leave from Institut für Festkörperforschung, KFA Jülich, Germany.
Reprints request to Dr. H. F. WENZL, Institut für Festkörperforschung, Kernforschungsanlage Jülich, *D-5170 Jülich 1*, Postfach 365.

[1] B. W. BATTERMAN u. H. COLE, Rev. Mod. Phys. **36**, 681 [1964].

[2] P. DEDERICHS, Phys. Rev. B **1**, 1306 [1970]. — F. W. YOUNG, T. O. BALDWIN, and P. H. DEDERICHS, in: Vacancies and Interstitials in Metals, ed. by A. SEEGER, D. SCHUMACHER, W. SCHILLING, and J. DIEHL, North-Holland Publ. Co., Amsterdam 1969.

[3] F. S. GOULDING, Nucl. Instr. Methods **43**, 1 [1966].

[4] W. H. ZACHARIASEN, Theory of X-ray Diffraction in Crystals, John Wiley, New York 1945.

[5] R. I. FOX, IEEE, Vol. NS-13, 367 (June 1966).

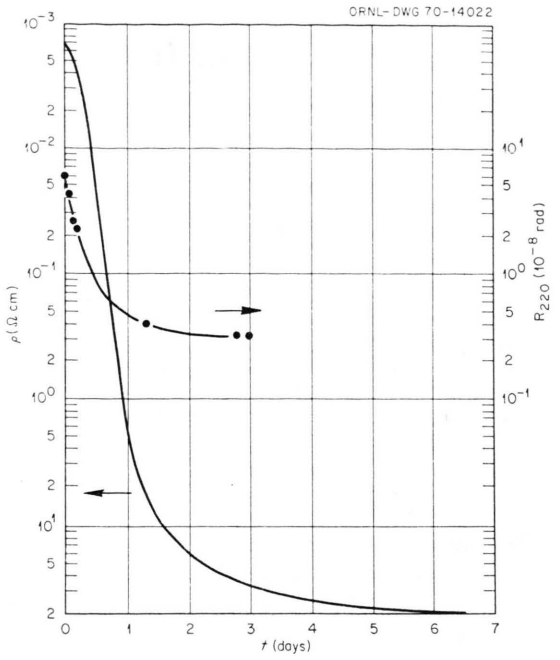


Fig. 1. Resistivity $\varrho$, as a function of time at room temperature, of a sample corresponding to sample 7 after doping at 425 °C with Li and quenching to room temperature [5]. Integrated X-ray intensity $R_{220}$, sample 7, after pulse heating (1 minute at 400 °C, partly re-solution of precipitates) as a function of time (precipitation at room temperature).

3 $HNO_3$)-solution at room temperature until sufficiently thin areas were obtained. Etch rates were 23 $\mu$m/min for lithium doped germanium.

The initial lithium content of the samples, taken as the equilibrium solubility concentration at the doping temperature of 425 °C, was about 30 ppm [6]. After annealing the samples about $^1/_2$ hour in vacuum near 550 °C, the Li content had dropped to 2 ppm, as revealed by a flame photometric analysis on sample 2 (10% accuracy; analysis by T. A. Carter, ORNL Analytical Chemistry Division). The oxygen content, as determined by Fox [5], was smaller than $10^{-3}$ ppm ($10^{14}$/cm$^3$) for samples 1, 2, 3, 7, and $10^{-2}$ ppm for sample 9 a.

The initial electrical resistivity was approximately 50 $\Omega$cm, n-type (4 years after doping). The dislocation density in the samples, determined by Borrmann topography [7] was between 500 and 1000 per cm$^2$.

## 3. GeLi Phase Diagram

The discussion of the effects during doping, precipitation and temperature treatment of the samples is based on the hypothetical phase diagram in Fig. 2, constructed from the information available, and analogous to the phase diagram of the SiLi system [6]. During doping at 425 °C one starts with a Li surface layer on the germanium crystal; the liquid lithium reaches local equilibrium with the germanium crystal by dissolving part of it, lithium diffuses into the bulk, compounds ($GeLe_3$ etc.) are probably formed, and ultimately equilibrium corresponding to an average lithium concentration of approximately 10% is reached. The overwhelming amount of Li is contained in the compounds and liquid, presumably at the surface of the specimen; only about 30 ppm are dissolved in the bulk as single lithium interstitials (see [8] for a survey of diffusion properties of Li in Ge, see [9] for discussion of retrograde solubility). After quenching to room temperature the lithium precipitates form $Li_3Ge$ particles (probably spherical) with a coherent phase boundary with the lithium matrix. The precipitation is probably nucleated by oxygen dissolved in the sample [10, 11].

After precipitation is finished at room temperature, further heating of the crystal in vacuum dissolves single lithium interstitials again, and the size and number of precipitates is reduced. Lithium may be evaporated from the surface. Therefore, a concentration gradient may build up in the sample if there is no activation barrier against outdiffusion [12]. Ultimately, all the Li should leave the sample. As will be shown, the x-ray method is capable of monitoring the decrease in size and number and the ultimate disappearance of the precipitates.

## 4. Measurements

The change of the effective absorption coefficient $\mu^*$ for the dynamic x-ray waves due to the lithium interstitials has been determined with several

[6] R. P. Elliott, Constitution of Binary Alloys, 1st Supplement, McGraw-Hill, New York 1965. 20 ppm according to chemical analysis.

[7] F. W. Young, T. O. Baldwin, A. E. Merlini, and F. A. Sherrill, Adv. X-ray Aalysis **9**, 1 [1966].

[8] C. S. Fuller and J. A. Ditzenberger, Phys. Rev. **91**, 193 [1953]. — A. Seeger and K. P. Chick, Phys. Stat. Sol. **29**, 455 [1968].

[9] R. G. Rhodes, Imperfections and Active Centers in Semi-Conductors, Pergamon Press, London 1964. — I. N. Hobstetter, Proc. Met. Phys. **7**, 1 [1958].

[10] R. D. Weltzin, R. A. Swalin, and T. E. Hutchinson, Acta Met. **13**, 115 [1965].

[11] Progress in Semi-Conductors, ed. by A. F. Gibson and R. E. Burgess, **7**, 127 [1963]; see also Vol. 2.

[12] M. H. Moore and P. H. Fang, J. Appl. Phys. **41**, 3447 [1970].

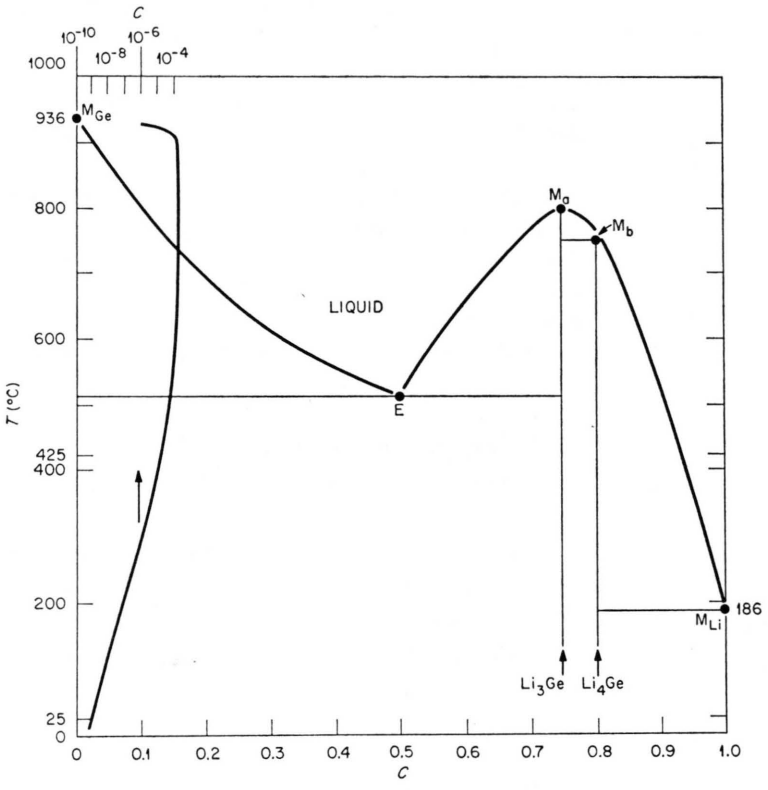


Fig. 2. Hypothetical phasediagram of GeLi, based on melting points of Ge($M_{Ge}$), Li($M_{Li}$), $Li_3Ge$($M_a$), $Li_4Ge$($M_b$), eutectic point $E$, solubility of lithium interstitials in germanium and distribution coefficient [6]. $C$ indicates the mole fraction of Li in the compound.

methods. At room temperature a double crystal spectrometer [13] was used with dispersion-free arrangements of the crystals in the Bragg-Laue scheme [4]. The integrated intensities [4] were determined for the symmetrical (220) reflection and transmission in Laue geometry, $R_{220}$, and for the symmetrical (333) reflection in Bragg geometry, $R^{B}_{333}$. The Borrmann "transmitted" and "reflected" intensity in Laue geometry were compared in a few cases and found to be equal, which indicates the absence of inhomogeneous strains in the samples [14].

The integrated intensity $R_{220}$ and the peak intensity $P_{220}$ of the symmetrical (220)-reflection for K$\alpha$ radiation in Laue geometry was measured as a function of temperature in an x-ray furnace on a Borrmann camera [15, 16]. It was assumed that [1] $P \sim R$.

From the measured integrated intensities $R$ the additional effective absorption coefficient, $\mu^*$, due to the presence of lithium, has been determined by comparison with the calculated value $R_p$ for the perfect crystal [17] using the parameters listed in Table 1. $R = R_p \exp(-\mu^* t_0/\cos\Theta)$, where $t_0$ denotes the sample thickness and $\Theta$ the Bragg angle. $\mu^*$ will be used in comparing experiment and theory. Figures 1 and 3 show results from specific experiments and Table 2 summarizes the significant data.

Preliminary measurements of the "integrated" diffuse scattering [18] in the wings of the (333)-Bragg-reflections in a $(3, -3)$ double crystal arrangement for the samples containing precipitates were not conclusive. The diffuse scattering intensity seems to be very small and more concentrated near the Bragg peaks compared with measurements on

[13] M. C. Wittels, F. A. Sherrill, and A. C. Kimbrough, Adv. in X-ray Analysis **7**, 265 [1964].
[14] B. Okkerse, Philips Res. Rep. **17**, 464 [1962].
[15] F. W. Young, Jr., T. O. Baldwin, A. E. Merlini, and F. A. Sherrill, Adv. in X-ray Analysis **9**, 1 [1966].
[16] T. O. Baldwin and J. E. Thomas, J. Appl. Phys. **39**, 4391 [1968].
[17] R. M. Nicklow, F. A. Sherrill, and F. W. Young, Jr., Phys. Rev. **137**, 1417 [1965].
[18] B. W. Batterman, Phys. Rev. **134**, 1354 [1964].

Table 1. X-ray data used for the calculations: $\lambda$=wavelength of characteristic K$\alpha$ radiaiton from copper, molybdenum, and silver; $\Theta$=Bragg angle in degrees; $\mu_0$=normal absorption coefficient; $\varepsilon_0 = f_{220}/f_0^{''}$, $F'_{220} = 22.8$=atomic scattering factor, $\Delta f'$, $f''$=Hoenl corrections [1]. Thermal Debye Waller factor for (220)-reflection at 300 °K: $\exp(-M) = 0.9697$.

| | | CuK$\alpha$ | MoK$\alpha$ | AgK$\alpha$ |
|---|---|---|---|---|
| | $\lambda$/Å | 1,542 | 0,711 | 0,50 |
| $\Theta$ | Ge 220 | 22,7 | 10,2 | 7,5 |
| $\Theta$ | Ge 111 | 13,2 | 6,2 | |
| $\Theta$ | 333 | 45 | 19 | |
| $\Theta$ | Cu 111 | 21,7 | 9,8 | 7,7 |
| | $\mu_0 \cdot$ cm | 350 | 325 | 165 |
| | $\varepsilon_0$ | 0,989 | 0,998 | |
| | $\Delta f_{220}$ | −1,3 | 0,2 | |
| | $f_{220}$ | 1,0 | 1,8 | |

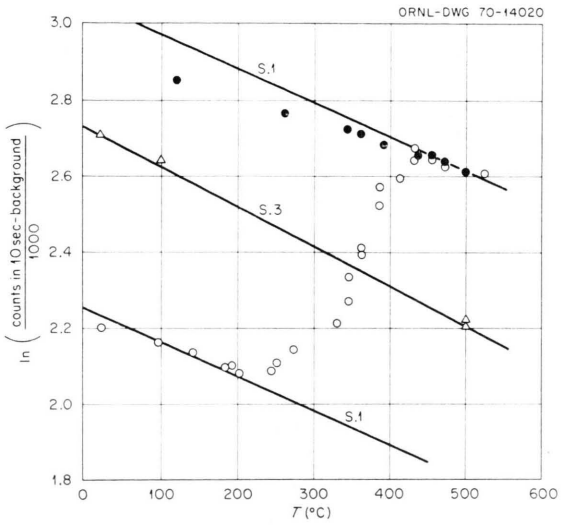


Fig. 3. Plot of peak intensity of symmetrical (220)-reflection in Laue geometry, using AgK$\alpha$ radiation, as a function of temperature. Samples heated in a vacuum of approximately $10^{-4}$ Torr. ○ Sample 1, first heating after doping with lithium and complete precipitation at room temperature; heating rate $\approx 2°$/min. ● Sample 1, cooling $\approx 4°$/min. Following this treatment, the integrated intensity remained essentially constant (over months), different from the behaviour in Fig. 1. △ Sample 3 (undoped), heated in same furnace (reference measurement; difference in absolute value and slope due to different thickness). Lines S.1 and S.3 indicate the calculated temperature dependence taking into acount changes of thermal vibrations only [17, 18].

neutron irradiated copper crystals containing small dislocation loops [19]. BATTERMAN reported a slight apparent increase in linewidth of the (333)-Bragg-reflection after precipitation [20]. One would therefore expect quite large precipitates with $r_p > 100$ Å.

Borrmann topographs, taken before and after the different treatments, did not reveal any changes in the dislocation pattern (resolution $\approx 5\,\mu$m). No precipitates could be resolved in the topographs, contrary, e. g., to the results on the GeAs system with a comparatively high content of arsenic [21]. Also, no precipitates could be detected in the electron microscope investigations of the doped samples, contrary to other reports [10]. Structures similar to those shown in [22] could be found, although mostly due to unspecified layers (dirt) on the surface of the specimen.

The experimental results, including those from other sources, can be summarized as follows:

a) Precipitation increases $\mu^*$ enormously.

b) Re-solution of the precipitates during heating of the doped samples can be observed easily as a decrease of $\mu^*$.

c) Short heating pulses lead to reversible behaviour, whereas prolonged heating in vacuum gives rise to an irreversible change of $\mu^*$, probably due to an outdiffusion of lithium.

d) Precipitation tends to increase the integrated intensity in Bragg reflection, as shown clearly by BATTERMAN [20].

e) Diffuse scattering seems to be concentrated near and under the diffraction peaks in Bragg geometry.

## 5. Discussion

The effects of defects and precipitates will be discussed on the basis of DEDERICHS' theory for the absorption of the coherent x-ray wave [2]. According to this theory, the lithium interstitials act essentially by displacing the lattice atoms, which gives rise to immediate additional photoelectric absorption and to elastic incoherent scattering of the coherent wave (elastic scattering absorption of coherent waves). In transmission, scattered waves ultimately are absorbed, too, except for a negligible fraction which emerges from a thin layer of approximately the thickness $1/\mu_0$ at the exit surface.

[19] P. H. DEDERICHS, T. O. BALDWIN, and J. E. THOMAS, to be published.

[20] B. W. BATTERMAN, J. Appl. Phys. **30**, 508 [1959].

[21] O. N. EFIMOV, E. G. SHEIKHET, and L. I. DATSENKO, Phys. Stat. Sol. **38**, 489 [1970].

[22] G. R. JINDAL and J. W. FAUST, JR., J. Appl. Phys. **41**, 2106 [1970].

$\mu^*$ can be related to a photoelectric absorption coefficient $\mu^{PE}$ and a diffuse scattering absorption coefficient $\mu^{DS}$ of the dynamical x-rays in transmission: $\mu^* = \mu^{PE} + \mu^{DS}$.

Values for $\mu^{PE}$ and $\mu^{DS}$ will be calculated, assuming the following model:

a) Random distribution of single lithium interstitials in the dissolved state with mole fraction $c = 30$ ppm (corresponding to maximum solubility at 425 °C).

b) Spherical precipitates with constant radius $r_0$.

c) Random distribution of precipitates with mole fraction $c_p$.

d) Constant concentration of lithium interstitials inside the precipitates: $c_0 \approx 3/4$, corresponding to a $GeLi_3$ phase. Then, $c_p = c\,v/(c_0\,4\pi\,r_0^3/3)$, where $v = 2.3 \cdot 10^{-23}\,\mathrm{cm}^3 = a^3/8$ denotes the atomic volume, $a = 5.66$ Å, the edge length of the unit cell.

e) The distortions by lithium interstitials are described in the elastic continuum approximation by the double force parameter $A$, which is related to the volume change $\Delta V$ due to the distortions by $\Delta V = 4\pi A \gamma$ (the factor $\gamma$ describes the surface effects in a finite sample [23]). Since $A$ for Li in Ge is not known, the value for Ni in Ge is taken [24]: $4\pi A/v \approx 0.1$.

Then for (220)-reflections, one gets:

$$\mu^{PE} = 24\,\mu_0\,c\,c_0\left(\frac{4\pi A}{v}\frac{r_0}{a}\right)^2 + \text{higher order terms} \approx \mu_0\,5{,}4 \cdot 10^{-6}\left(\frac{r_0}{a}\right)^2 \tag{1a}$$

if $(4\pi A/v)\,(r_0/a)\,c_0\,6{,}3 < 1$ ("small" precipitates),

$$\mu^{PE} \approx 15{,}1\,\mu_0\,c\,c_0^{1/2}\left(\frac{4\pi A}{v}\frac{r_0}{a}\right)^{3/2} \approx \mu_0\,2{,}1 \cdot 10^{-5}\left(\frac{r_0}{a}\right)^{3/2} \tag{1b}$$

if $(4\pi A/v)\,(r_0/a)\,c_0\,6{,}3 > 1$ ["large" precipitates; Equ. (36) in [2]].

$$\mu^{DS} = A \cdot 10^3\,\mathrm{cm}^{-1}\left(\frac{\lambda}{a}\right)^2\left(\frac{4\pi A}{v}\right)^2\left(\frac{r_0}{a}\right)^3 c\,c_0 \cdot \cos^2\Theta \cdot \ln\left(\frac{2000}{r_0/a}\right)$$

$$= B \cdot 10^4\,\mathrm{cm}^{-1}\left(\frac{\lambda}{a}\cos\Theta\right)^2\left(\frac{r_0}{a}\right)^3 \ln\left(\frac{2000}{r_0/a}\right), \tag{2}$$

where $A = 1{,}2$, $B = 2{,}6$ for copper, $A = 1{,}3$, $B = 2{,}9$ for molybdenum and silver radiation.

Both $\mu^{PE}$ and $\mu^{DS}$ increase stronger than linearly with the radius $r_0$ of the precipitates, as long as $r_0 \ll$ extinction length[2] $\approx 2000$ a. The effective absorption coefficient due to dissolved lithium is so small that it has been neglected in the formulae, which describe here only effects due to the enhanced lattice distortions by the "coherent" action of lithium in the precipitates.

In addition to the x-ray parameters, Equations (1) and (2) contain $r_0$ as the only unknown; thus it can be determined from experimental values for $\mu^{DS} + \mu^{PE} = \mu^*$. By comparing the results for different x-ray wavelengths the consistency and applicability of the theory can be checked.

$\mu^{PE}$ depends on the normal absorption coefficient $\mu_0$. $\mu^{PE}$ can be related to a quasi (static) Debye Waller factor $L$: $\mu^{PE} = \mu_0 L$, where $L \sim c\,A^2_{\mathrm{eff}}$. It is the quadratic dependence on the effective distortion field parameter $A_{\mathrm{eff}}$, related to single defects or precipitates, which gives rise to the enormous enhancement of $\mu^{PE}$ by clustering ($c \to c/n$, $A_{\mathrm{eff}} \to n\,A_{\mathrm{eff}}$, $L \to n\,L$, where $n$ denotes the number of defects in the cluster). By comparing experimental values of $\mu^*$ for different wavelengths, $L$ can be determined without having to assume constant $r_0$ for all precipitates, because it is not necessary here to know $r_0$ explicitly before being able to calculate $L$. Equality of both values of $L$, one calculated after having determined $r_0$ from Equations (1) and (2), the other by this method, would confirm the validity of the assumption of constant $r_0$ for all precipitates.

$\mu^{DS}$ is independent of $\mu_0$, but depends in a similar way on $c\,A^2_{\mathrm{eff}}$ as $\mu^{PE}$. The diffuse scattering due to defects can be determined directly in Bragg geometry. There, the measured integrated intensity $R^B$ is related to the static Debye Waller factor $L$, the integrated intensity for a perfect crystal,

[23] J. D. Eshelby, Solid State Physics, Vol. 3, ed. by F. Seitz and D. Turnbull, Academic Press, New York 1968.

[24] N. E. Moyer and R. C. Buschert, Radiation Effects in Semiconductors, ed. by F. L. Vook, Plenum Press, New York 1968.

$R_p^B$, and a mosaic crystal, $R_m^B$: [19]

$$R^B = R_p^B e^{-L} + R_m^B (1 - e^{-2L}). \quad (3)$$

The second term describes the integrated diffuse scattering. The relation allows a direct determination of $L$. It is not valid for too large precipitates, for which the diffuse scattering tends to be concentrated below the ,Bragg peak, where it is reduced due to dynamical effects ("primary extinction").

Figure 4 shows graphs of Eqs. (1) and (2), including points calculated by using data from former electron microscope investigations [10].

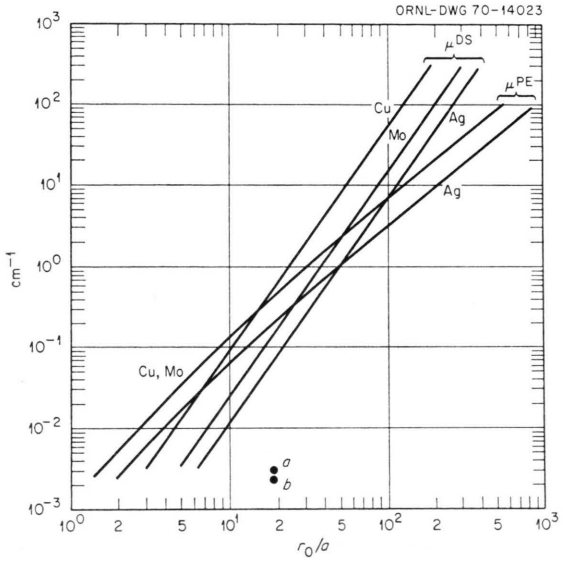


Fig. 4. $\mu^{DS}$ and $\mu^{PE}$ as a function of $r_0/a$ according to Eqs. (1) and (2). Parameters: characteristic Kα radiation from different elements. $a$ and $b$ indicate values for $\mu^{PE}$ and $\mu^{DS}$, respectively, corresponding to the data given in [10], namely: $c = 1$ ppm (probably too small for the doping temperature used), $c_p = 5 \cdot 10^{-5}$ ppm, $\varepsilon = 10^{-3}$, $c_0 = 0.1$, volume of precipitates $V_p = c\, v/c_p\, c_0 = 2 \cdot 10^5\, v$; assumption: $4\pi A/v = 30\, \varepsilon$ (lithium distortion fields are additive).

## Results

a) By inserting experimental values in the equation $\mu^*_{exp} = \mu^{PE} + \mu^{DS}$ one can determine the radii of the precipitates, and then $\mu^{PE}$ and $\mu^{DS}$ separately. For the samples with small oxygen content one gets typically (copper radiation, sample 2): $\mu^*_{exp} \approx 56\,cm^{-1}$, $r_0/a \approx 100$, $\mu^{PE} \approx 7\,cm^{-1}$, $\mu^{DS} \approx 49\,cm^{-1}$. For sample 9 a with the large oxygen content one gets for copper radiation: $\mu^*_{exp} \approx 10\,cm^{-1}$, $r_0/a \approx 50$, $\mu^{PE} \approx 2\,cm^{-1}$, $\mu^{DS} \approx 8\,cm^{-1}$. The dependence of $\mu^*_{exp}$ on wavelength (Table 2) is in agreement with Eqs. (1) and (2) and mainly due to the strong dependence of $\mu^{DS}$ on wavelength. The difference in precipitate radius for samples 2 and 9 a confirms the assumption that the precipitates are nucleated by oxygen impurities [25].

b) For comparison with Eq. (3) one can calculate the exponent in the static Debye Waller factor $L$ from the transmission experiments: $L_{220} \approx \mu^{PE}/\mu_0 \approx 2/350 \approx 6 \cdot 10^{-3}$ for sample 9 a and copper radiation. By comparing the values of $\mu^*$ for copper and molybdenum radiation, using Eqs. (1) and (2), one gets a slightly different value: $L_{220} \approx 27 \cdot 10^{-3}$. This value is more reliable, because it is not based on the assumption of constant $r_0$. The difference in these two values of $L_{220}$ indicates that the distribution of precipitate radii is not as sharp around $r_0$ as assumed. Inserting Batterman's results for Bragg geometry [20] ($R^B_{333} = 2{,}6 \cdot 10^{-5}$ rad, $R^B_{(333)m} = 7{,}8 \cdot 10^{-5}$ rad, $R^B_{(333)p} = 2{,}1 \cdot 10^{-5}$ rad) into Ep. (3), one calculates $L_{333} = 37 \cdot 10^{-3}$, which corresponds to $L_{220} \approx (27/8) \cdot L_{333} = 12 \cdot 10^{-3}$. Both values of the static Debye Waller factor, determined from transmission and reflection experiments, are of the same order of magnitude showing the consistancy of the model used.

Whereas Batterman has explained the increase of the integrated intensity in Bragg geometry due to the precipitates in the otherwise perfect sample by a decrease of the "primary extinction", the above arguments suggest that it is caused mainly by an enhanced scattering intensity, which is concentrated near the Bragg peaks. The diffuse scattering even tends to become smaller at the center of the peak due to primary extinction effects.

c) The data of HUTCHINSON et al. [10] lead to values of $\mu^*$ which are several factors of ten too small (Fig. 4) to be able to explain the x-ray absorption.

d) The decrease of $\mu^*$ (which ultimately vanishes) by thermal treatments (Figure 4, Table 2) and the result of the chemical analysis show that lithium can leave the sample. For a particular treatment leading to a certain change of $c$ and $r_0$, the corresponding change in $\mu^*$, $\Delta\mu^*$, depends on the wavelength of radiation used. It can be shown (by differentiating Eqs. (1) and (2) with respect to $r_0$ and $c$) that

$$\frac{\Delta\mu_1^*}{\Delta\mu_2^*} \approx \frac{10^5 (\lambda_1/a)^2 + \mu_{01}\,cm}{10^5 (\lambda_2/a)^2 + \mu_{02}\,cm}.$$

[25] J. R. CARTER and R. A. SWALIN, J. Appl. Phys. **31**, 1191 [1960].

Table 2. Survey of experimental results. The integrated intensity in symmetrical Laue geometry [1] is given by $R=E\,\omega/I_0$, where $E$ is the total number of counts above background measured during rocking the crystal over the (220)-diffraction maximum with angular velocity $\omega$, $I_0$ is the X-ray intensity (counts per unit time), entering the part of the crystal under investigation. DB indicates that also the monochromator crystal was used in Laue and not, as usual, in Bragg geometry. $p$ denotes intensities of the 220-peak in Laue geometry, $R^B$ integrated intensities in Bragg geometry for (333)-reflection. Error: the maximum relative deviation from the mean value of $R$ in several experiments was 10% or less. The sample thickness was always so large that the primary beam was essentially absorbed ($\mu_0 t_0 \gg 1$).

| Crystal Number | Thickness $t_0/\mu$m | Treatment | CuKα $R/10^{-8}$ rad (except $R^B$) experiment | CuKα theory | $\mu^*\cdot$cm | MoKα $R/10^{-8}$ rad exp. | MoKα theory | $\mu^*\cdot$cm | AgKα exp. | $\Delta\mu^*$cm |
|---|---|---|---|---|---|---|---|---|---|---|
| 1 | 540 | | 0,55 | 96 | 89 | | | | $p^{1\prime}/p^1 \approx 2{,}1$ | 14 |
| 1′ | 540 | heated to 600 °C (2°/min) then cooled (4°/min) to 300 °K | 32 | 96 | 19 | | | | | |
| 1″ | 410 | | 55 | 140 | 29 | 66 | 107 | 12 | | |
| 2 | 640 | | 1,6 | 77 | 56 | | | | $p^{2\prime}/p^2 \approx 3{,}0$ | 17 |
| 2′ | 640 | as 1′ | 16 | 77 | 23 | | | | | |
| 3 | 650 | undoped | 85 | 76 | $< 0$ | | | | | |
| 7 | 800 | | 0,22 | 54 | 64 | | | | $R^{7\prime}/R^7$ W 2,0 | |
| 7′ | 800 | as 1′ | 2,8 | 54 | 34 | | | | | |
| 7′ | 800 | 100 h later | 4,6 | 54 | 28 | | | | | |
| 7″ | 580 | thinned by etching | 17 | 91 | 29 | | | | | |
| ″ | 580 | | $R^B = 2{,}2\cdot10^{-5}$ | $2{,}1\cdot10^{-5}$ rad | | | | | | |
| 7″ | 580 | 2 mos. after heating 7′ | 11 | 91 | 36 | 27 | 67 | 15 | | |
| 7‴ | 580 | 10 min, 800 °C $10^{-5}$ Torr | 180 (DB) | 150 | $< 0$ | | | | | |
| 7‴ | 580 | 24 h later | 150 (DB) | 150 | $\approx 0$ | | | | | |
| 9a | 470 | $2\cdot10^{15}$ 0/cm³ | 71 | 120 | 10 | 65 | 86 | 5,7 | | |

For sample 2 and comparing CuKα and AgKα radiation one calculates $\Delta\mu^*_{Cu}/\Delta\mu^*_{Ag} \approx 2{,}7$, which is of the same order as the corresponding experimental value of 1,9 (Table 2).

e) Diffusion length $l_D$ can be calculated from the diffusion coefficient [8] and the time and temperature necessary for complete removal of the lithium. For the case of sample 7 (Table 2) one gets a reasonable value of $l_D \approx 1$ mm, a factor of 2 larger than the thickness of the sample.

## 6. Conclusion

It has been shown that the effective absorption coefficient of dynamical x-ray waves in a nearly perfect crystal indicates precipitation and re-solution of precipitates sensitively, and that the effects can be interpreted by using Dederichs' theory.

Our results suggest that germanium crystals, to be used e. g. for particle detectors, can be characterized as far as diffusion and precipitation of lithium is concerned by doping them with lithium, measuring the precipitation effects by anomalous x-ray transmission, and eventually removing the lithium again by suitable heating procedures. Even detectors themselves could be tested, although the lithium concentration there is about a factor of 100 smaller than in our samples, corresponding to $\mu^* < 1\ \mathrm{cm}^{-1}$, if the lithium is precipitated.

Generally, as soon as nearly perfect crystals can be obtained, dynamical diffraction can be used as a sensitive probe for the spacial distributions of crystal lattice constituents, which give rise to distortions, even if the corresponding structures are too small to be resolved in x-ray topographs.

*Acknowledgements*

I thank R. Fox and R. Westbrook for providing samples and for help during sample preparation, and D. Miller, who searched for precipitates in the electron microscope and who provided the recipes for preparing the microscope samples. Special thanks are due to P. Dederichs, B. C. Larson, G. Leibfried, T. S. Noggle, F. A. Sherrill, and F. W. Young, Jr. for help in the experimental work and for many clarifying discussions. I am grateful to F. W. Young, Jr. for a thorough reading of the manuscript and, generally, for providing a stimulating and critical atmosphere for research.